Accepted Manuscript

Title: Using Computational Fluid Dynamics in the Forensic Analysis of a Prison Fire

Author: Wolfram Jahn Orelvis Gonzalez Juan de Dios Rivera José Luis Torero

Please cite this article as: Wolfram Jahn, Orelvis Gonzalez, Juan de Dios Rivera, José Luis Torero, Using Computational Fluid Dynamics in the Forensic Analysis of a Prison Fire, *Forensic Science International* (2015), http://dx.doi.org/10.1016/j.forsciint.2015.06.003

This is a PDF file of an unedited manuscript that has been accepted for publication. As a service to our customers we are providing this early version of the manuscript. The manuscript will undergo copyediting, typesetting, and review of the resulting proof before it is published in its final form. Please note that during the production process errors may be discovered which could affect the content, and all legal disclaimers that apply to the journal pertain.

Acknowledgments

1

Using Computational Fluid Dynamics in the Forensic Analysis of a Prison Fire

Wolfram Jahn[a], Orelvis Gonzalez[b], Juan de Dios Rivera[a], José Luis Torero[c]

[a]*Pontificia Universidad Católica de Chile, Department of Mechanical and Metallurgical Engineering*
[b]*Ingeniería DICTUC S.A.*
[c]*The University of Queensland, School of Civil Engineering*

Abstract

On the 8th of December of 2010 a fire killed 81 inmates in a Chilean prison. While the collected evidence (including eye witness accounts) indicated an intentional fire, started by a group of inmates who were fighting against another group and who ignited a mattress and threw it over a bunk bed inside the cell, it could not be established how fast the fire grew and whether the prison guards acted promptly enough to prevent the tragedy. In this context, the public defender office in charge of the case requested an independent investigation in order to determine the approximated time the fire started, and the temperature evolution of the padlocks at the cell doors during the initial stage, based on the construction characteristics of the prison, the existing materials and the evidence collected during the investigation. Computational Fluid Dynamics (CFD) were used to analyse the movement of the smoke and to match the first appearance of smoke on CCTV recordings at locations away from the fire, allowing for the recreation of the time-line of events. The padlock temperatures as a result of hot gases from the fire was also simulated. It was shown that the fire grew quickly and became uncontrollable before the guards could intervene. By the time the guards arrived at the cells' door, the padlocks were shown to be too hot to be handled without protection.

Email address: wjahn@ing.puc.cl (Wolfram Jahn)

Highlights

- The time to ignition of a prison fire was estimated based on smoke appearance on CCTV cameras using CFD modelling

- Laboratory experiments were conducted to establish the rate of heat release

- Padlock temperatures at cell doors were estimated from simulations.

1

Abstract

On the 8th of December of 2010 a fire killed 81 inmates in a Chilean prison. While the collected evidence (including eye witness accounts) indicated an intentional fire, started by a group of inmates who were fighting against another group and who ignited a mattress and threw it over a bunk bed inside the cell, it could not be established how fast the fire grew and whether the prison guards acted promptly enough to prevent the tragedy. In this context, the public defender office in charge of the case requested an independent investigation in order to determine the approximated time the fire started, and the temperature evolution of the padlocks at the cell doors during the initial stage, based on the construction characteristics of the prison, the existing materials and the evidence collected during the investigation. Computational Fluid Dynamics (CFD) were used to analyse the movement of the smoke and to match the first appearance of smoke on CCTV recordings at locations away from the fire, allowing for the recreation of the time-line of events. The padlock temperatures as a result of hot gases from the fire was also simulated. It was shown that the fire grew quickly and became uncontrollable before the guards could intervene. By the time the guards arrived at the cells' door, the padlocks were shown to be too hot to be handled without protection.

1. Introduction

There have been several fires in Latin-American prison facilities in the last decades, many of them accompanied by important loss of life. Among the most important events range the fire occurred in Honduran Comayagua prison in February of 2012, which killed 361 people, the fire in Higey prison, Dominican Republic, where 136 people died on the 7th of March 2005, and the fire in San Pedro Sula prison, also in Honduras, with 101 dead inmates in early 2004 [1]. A common factor in all these events is overcrowding and critical living conditions existing in the prisons. In Chile the most important prison fire took place on the 8th of December 2010 at San Miguel prison in the country's capital Santiago,

1

where 81 inmates were killed. In the present document it is illustrated how experimental tests together with Computational Fluid Dynamics modelling were used to correlate evidence from the beginning of the fire to the appearance of smoke in the CCTV recording at the other side of the building, thus recreating the time-line of critical events.
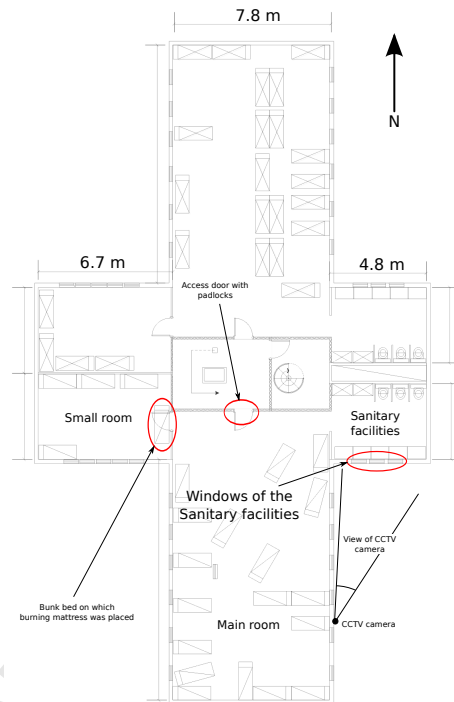

Figure 1: Layout of the prison floor

San Miguel prison has a somewhat different layout from what is used in most developed countries; instead of having cells shared by two or three inmates, distributed along a corridor, this prison consists of five four-storey blocks, each having a central staircase with large open plan floors (see figure 1). The floors are divided into two equal (mirrored) rooms, separated from the staircase by bars. Each room has a smaller cell attached, which is accessed from within the room through a barred door. Across from the room are located the common sanitary facilities. Figure 2 shows an external view of the prison block affected

2

by the fire. The three windows to the right correspond to the sanitary facilities on each floor, while the six windows correspond to the large common room. All windows are covered with metallic louvres (but no glass). On the top floor the soot marks from the smoke are still visible.

Figure 2: External view from north-east of Block 5 of San Miguel's prison. This photograph was taken a few days after the fire. The CCTV camera that captured the smoke coming out of the windows of the sanitary facilities on the day of the incident can be seen in the upper part of the image.

Inmates use their bunk beds, sheets and blankets to create semi-closed spaces shared by six to nine people (see figure 3(a)). In order to prevent air currents entering the cell, they hang blankets on the barred walls and across the open doors of the sanitary facilities. Personal belongings are stored in self-made over-head compartments between the concrete beams, as shown in figure 3(b). In those compartments they keep clothes, magazines, newspapers and other items, most of them made of combustible materials.

The prison of San Miguel is used for remand detention, and as such allows its inmates certain level of autonomy. Among other things they are allowed to brew their own tea, for which they are provided gas burners and LPG.

3

(a) Bunk beds with hanging sheets and blankets.

(b) Over-head compartments.

Figure 3: Internal view of a typical cell at San Miguel's prison

At the time of the incident, the room where the fire started—which is located on the fourth floor—housed 71 inmates on a total surface area of about 160 m^2 including the bathrooms. The mirror room located across the staircase had the same area and housed 75 inmates. The little cell attached to the main room usually is occupied by the more influential inmates (of higher hierarchy), as it provides certain level of privacy. The barred doors communicating the main rooms to the staircase are locked by two padlocks, one at 0.5 m above the floor and another one at about 2 m above the floor. The prison block is made of reinforced concrete and is four floors high, each one having the same layout described, and is accessed through an underground tunnel. During nights no guards are placed within the prison block. Therefore, in order to access the cells on the fourth level, the guards had to walk across the tunnel, opening several doors before climbing the stairs and finally opening the two padlocks placed on each cell door.

The accusation against the guards on duty, that led to prosecution, was that they acted negligently by ignoring the fire for a prolonged period of time (over half an hour), allowing it to grow out of control.

4

During the prosecution process of this case, two important issues needed to be analysed: Firstly, the maximum time elapsed between the moment a self-sustained fire was burning in the cell, and the first appearance of smoke on CCTV recordings at locations away from the fire needed to be established, which would allow for the recreation of the time-line. Secondly, it was required to analyse the temperature evolution of the padlocks present at the cell doors, in order to sustain (or refuse) the claim of the prison guards that they were not able of handling them without protection.

This information was of utmost importance for determining whether or not the guards could have arrived and intervened at the fire before it grew uncontrollable, in order to evacuate the inmates safely.

2. Case history

According to witness' accounts, in the early hours of the 8th of December a group of inmates of the southern room on the fourth floor started a row. Surviving inmates stated that there were two opposing factions; the occupants of the little cell on one side, and some of the occupants of the main cell on the other. During the course of the fight, the occupants of the little cell put a bunk bed in the entrance to block their adversaries attacks. Later, the occupants of the main cell used a handmade gas torch (connected to a LPG cylinder) to ignite a polyurethane foam mattress, which they threw onto the lower level of the bunk bed blocking the access of the little cell. In order to prevent their locked-in opponents from extinguishing the fire, they kept them at a distance using long wooden sticks with sharp tips (presumably made from knives and other metallic objects). The fire spread across the burning mattress and ignited other combustible objects, such as sheets, blankets and combustible items in the over-head compartments, resulting in an uncontrollable fire in a relatively short time. The large amount of combustible material, and its favourable geometrical configuration combined with a continuous supply of fresh air (the blankets covering the bars between staircase and the cell were rapidly consumed), in-

5

evitably resulted in a substantial fire that quickly had grown far beyond the extinguishing capability of the inmates.

Figure 4: Post-fire internal view of the small room where the fire started.

The guards stated that they gave notice to the fire services once they had seen smoke on the CCTV cameras pointing towards the windows of the sanitary facilities. Simultaneously a group of guards headed for the fourth floor (arriving there two or three minutes later). According to their testimony, by the time they arrived at the location of the fire, the padlocks of the prison block were too hot to be handled without protection, which made evacuation impossible, causing the death of nearly all of the occupants of that room.

In figure 4 a photograph of the small room after the fires is shown. The complete destruction caused by the fire is evident.

3. Methodology

The collection of evidence at the scene of the incident provided little insight into the sequence of events that evolved into the tragedy at hand. From witnesses' testimonies it can be conclusively stated that the fire was started intentionally by a group of inmates. It can further be assumed that the fuel

6

load present in the cell at the time of the incident was very similar to what the authors saw in other cells during their visit to the prison a few months later (see figure 3). But estimates made by inmates as to how long the fire had burned before the first guards arrived at the scene and tried to rescue the inmates are contradictory and cannot be treated as trustworthy. At 06:50 AM, CCTV recordings show smoke coming out of the bathroom windows at the fourth floor (an image of the bathroom windows as viewed by the camera a few days after the fire is shown in figure 5). This is the first (and only) tangible sign of the fire, and the methodology presented in the following sections is used to estimate the time of ignition, based on experiments and computational modelling of fire dynamics and smoke movement.

Figure 5: View angle of the CCTV cameras that captured the smoke coming out of the windows of the sanitary facilites.

Given the large amount of uncertainties present in the problem, it was necessary to establish a methodology conservative enough to account for the variability in the assumptions. An informal assessment of fuel density and configuration suggested that the fire must have grown to untenable conditions in a relatively short period of time. Thus it was decided to estimate the maximum amount of time it could have taken the fire to establish in the small room and the smoke to

7

travel across the main room and be detectable in the CCTV recordings, under any rational assumptions that fit the evidence.

In order to estimate the spread rate of the fire, and thus the time it took the fire to establish itself, a set of laboratory tests were conducted. The curve of the rate of released heat, extracted from those experiments, was then input into a computer model to simulate the smoke movement across the room and its detection with CCTV cameras outside the bathroom windows. An estimate of the time of ignition was finally obtained by subtracting the overall time (smoke production plus travel time) from the moment of smoke appearance in CCTV recordings.

4. Fire Dynamics

Fire results from the complex interaction of several physical processes, linked together through a positive feedback cycle; radiation from the flames heats up the surface of the (solid) fuel, triggering the release of volatile vapours at a rate that depends, among other factors, on the heat transfer into the solid. The freed volatiles are dragged into the combustion zone by convective forces and react with the oxygen, that diffuses towards the combustion zone from the surrounding air. The heat released in the combustion is then partially radiated back to the surface, completing the cycle [2].

Within a compartment, a fire is initially fuel-controlled, i.e. the height of the flame and the fire's energy release depend mainly on the available (gaseous) fuel. As the fire grows, the availability of oxygen starts to decrease locally, so that combustible gases must travel longer distances to find enough oxygen to burn. This results in ever longer flames, which in turn irradiate heat to surfaces farther away. Eventually flashover occurs when volatiles from remote surfaces ignite, converting the once localised fire into a generally burning volume that engulfs the entire compartment. Fire dynamics are fundamentally different once flashover has occurred, and must be analysed separately from the initial stage.

The most important parameter to be established in a fire is its heat release

8

rate (HRR) [3],

$$\dot{Q}_c = \chi \Delta h_c \dot{m}_f, \tag{1}$$

where $\dot{m}_f$ represents the burning rate, χ the combustion efficiency, and Δh_c the heat of combustion of the fuel. In a fuel controlled fire the burning rate is function of the fire area $A(t)$ and a constant rate of pyrolysis $(\dot{m}_f'')$,

$$\dot{Q}_c(t) = \chi \Delta h_c \dot{m}_f'' A(t), \tag{2}$$

The three constant properties can be summarised in a single parameter, the HRR per unit area (HRRPUA $\equiv \chi \Delta h_c \dot{m}_f''$). While HRRPUA is a material property, that can be obtained from a calorimetric test [4], the growth of the fire area, $A(t)$, depends on the fuel configuration and the amount of radiation received from the flame. After flashover has occurred, the fire is no longer fuel controlled, and the HRR depends exclusively on the supply of oxygen in the fire compartment. Heselden et al. propose the following correlation between HRR and ventilation conditions [5],

$$\dot{Q}_c = \beta \Delta h_c A_v \sqrt{H_v}, \tag{3}$$

where A_v is the overall area of openings of the compartment, H_v is the average height of openings, and $\beta = 0.09$ kg/s·m$^{5/2}$ is an experimental constant. It is important to note that $\dot{Q}_c$ in equation (3) considers the total HRR, resulting from both internal and external flaming. For the small room, considering closed windows and a frontal opening with an area of 1.9 m^2, the post-flashover maximum HRR obtained from equation (3) is about 2.4 MW (assuming that all fuel is made of polyurethane foam with a heat of combustion of 9600 kJ/kg [2]).

4.1. Estimates of Main Fire Characteristics

Before undertaking more complex computational simulations, the main fire characteristics were estimated from simple models.

Smoke movement is driven by temperature induced density gradients, resulting from the combustion of the fuel present in an enclosure. In the absence of

9

external forces, such as wind, smoke rises to the ceiling of the enclosure, expanding horizontally from the point of impingement of the plume until it encounters the surrounding walls. Limited by the enclosure, the smoke thus tends to form a relatively homogeneous hot layer that descends according to the volume of smoke produced by the fire. In large compartments with a simple geometry this can be modelled to an acceptable degree of accuracy using a two-zone approach [6, 7], where the compartment is divided into a hot upper layer, and a cool lower layer. The main variables of interest are the upper layer temperature and the height of the upper layer as a function of time. Zone models can help to give an overall idea of time-frames and temperature ranges. The moment the smoke layer reaches the height of the burning object can be used as a proxy for the occurrence of flashover (following from [8, 9]). Using this approach, flashover was estimated to have happened after about 170 s.

In order to estimate the average post-flashover temperature in the small room, simple energy balance of the fire compartment is cast,

$$\dot{Q}_c = \dot{Q}_L + \dot{Q}_R + \dot{Q}_{\mathrm{cond}}, \tag{4}$$

where $\dot{Q}_L$ and $\dot{Q}_R$ refer to flow of hot gases out of the compartment and radiative losses respectively, and $\dot{Q}_{\mathrm{cond}}$ stands for heat losses due to conduction into walls. A detailed account of how the different heat losses are calculated can be found in [2], and it suffices to state that all losses are a function of the temperature inside the fire compartment. Following the procedure outlined in [2], equation (4) an estimate of the temperature inside the compartment can be obtained (this has to be done iteratively, due to the non-linear nature of the resulting equation). For the compartment at hand (about 95 m^2 of internal surface, and concrete walls 0.1 m thick), with a maximum HRR of 2.4 MW, the post-flashover temperature estimate is around 750°C. It is conjectured that actual temperatures within the small room were lower, as an important part of the burning probably occurred outside the small room, and thus did not contribute to equation (4). This was confirmed by the CFD simulations.

10

5. Computer Modelling

In complex geometries, and under the influence of external factors (e.g. wind) the movement and distribution of smoke in a fire is much more complicated than what can be captured by a two-zone model, and more sophisticated tools must be used for analysis [10].

Computational Fluid Dynamics (CFD) is a numerical technique that outputs the flow field within a certain control volume, providing insight into flow velocities, spatial temperature distributions and pollutant concentrations within the volume. For this purpose the partial differential equations that govern the flow are discretised on a numerical mesh, resulting in a large set of linear equations that can be solved using standard computational routines [11]. The governing equations (known as Navier-Stokes equations) are non-linear and relatively complex in nature, not allowing for a general solution that can be universally applied. There are several commercial software packages that implement CFD, most of which are specifically tailored for a certain set of applications with simplified governing equations that can be solved with an acceptable level of use of resources. The simulation of compartment fires posts special challenges for CFD, as physical phenomena at very different length- and time-scales need to be addressed, and resource intensive sub-models are of primordial importance (e.g. radiation) [10].

While the use of computational models to simulate fire dynamics is relatively common for design purposes, it is less common for forensic analysis (see for example [12]). This is partially due to the inherent uncertainties associated with setting up the computational model, which result in relatively large variability in the outcome. For the simulation output to be useful in forensic analysis, the model must be set up in a manner such that its limitations and the input uncertainties do not affect the conclusions drawn from the results [13].

5.1. Fire Dynamics Simulator (FDS)

The software package used in this analysis is FDS in its version 5 (FDSv5) [14]. FDSv5 solves a simplified version of the Navier-Stokes equations, adequate for

11

buoyancy driven, slow flows (as is smoke). The solver uses a Large-Eddy-Simulation (LES) approach to treat turbulence flow, where eddies at length scales bigger than grid size are directly solved, while the dissipative process of eddies at sub-grid level are approximated using Smagorinsky's approach [15, 16]. Equations are spatially discretised using a finite-differences approach on a rectangular grid. Time dependency is solved using an explicit second-order Runge-Kutta scheme, where the time step is automatically adjusted so that the Courant-Friedrichs-Lewy condition is met. Radiation is included in FDS via the radiation transport equation for a grey gas, which is solved using a finite volume technique. While FDS features a simple gas-solid interaction model, heat transfer into physical boundaries is only one-dimensional and thus accurate predictions of surface temperatures have to be analysed carefully. FDS has been extensively validated for flow fields and temperature distributions for prescribed HRR curves [17, 18]. This validation ensures that the underlying equations are correctly solved, but it does not ensure that the model's output inherently represents reality. An adequate set-up of a CFD fire model requires that boundary and initial conditions are applied in a correct manner, taking into account the specific scenario and the limitations of the model. The process of defining the model parameters in the case under analysis is described in the following sections.

5.1.1. Modelling the Heat Release of the Fire

FDS includes a relatively simple combustion model that allows for the simulation of heat released in a fire for a given rate of combustible gas injection (according to a prescribed function). Although it is in principle possible to calculate the heating and subsequent pyrolysis of surrounding objects in order to simulate fire growth, the numerical resolution in the combustion zone is generally not fine enough in order to provide trustworthy predictions of the heat transferred to the surface, thus resulting in wrongly calculated growth rates [19]. Studies have also shown that blind predictions of fire growth, i.e. predictions that are not compared to data at intermediate stages, result in large discrepan-

12

cies, invalidating the outcome [20]. It is therefore recommended to implement the HRR as a prescribed function of time, obtained from laboratory experiments [21]. If other pertinent parameters are correctly set, FDSv5 will then adequately compute the movement of the smoke impelled by the fire, yielding flow field and temperature distributions within the smoke [22].

For the reasons exposed in the previous paragraph, the HRR in this analysis is not a result of simulations, but is an input into the CFD model. The HRR curve, obtained from laboratory testing, describes how energy is released by a certain fuel in a certain configuration as a function of time. Rather than prescribing the HRR as an energy inflow into the computational domain, FDSv5 requires the user to specify the rate of injection of a combustible gas into the domain, that will react releasing the prescribed energy when the air-fuel mix reaches stoichiometric conditions. This allows for a spatial temperature distribution within the compartment. The gas injection is prescribed by specifying the parameters of equation (2); a constant rate of pyrolysis $\dot{m}''_f$, a growing fire area ($A(t)$) and the heat of combustion. These parameters have to be determined from laboratory testing.

During the fully developed stage (ventilation-controlled), the maximum burning rate—given by equation (3)—is prescribed, and the HRR is calculated by FDS according to the supply of oxygen to burn the prescribed volatiles.

5.1.2. Mesh Size

Mesh size is a fundamental factor in numerical simulations of physical phenomena. The accuracy of the solution strongly depends on the size of the cells into which the computational domain is divided in order to discretise the governing partial differential equations. The discrete solution approaches the exact solution as cell volumes approach zero. For practical applications, however, it is necessary to trade numerical accuracy for computational resources. An adequate mesh size can be found by comparing the solution obtained with several different mesh sizes; once the improvement in accuracy by refining the mesh is not justified by the additional computing time, and acceptable mesh size is

13

found. In FDSv5, a rectangular structured mesh can be prescribed. It has been shown to yield good agreement with experiments for cell sizes of 8–15 cm, although the resolution must be considerably higher for a good agreement close to the burning region [23, 24].

In the present analysis the main focus lies on smoke movement and temperature, and a detailed simulation of the flame structure—which would require mesh refinement in the small room—is not necessary. Therefore a uniform grid with a cell size of 10 cm and no local refinement was adopted, resulting in about 3 million grid cells.

5.2. Padlock Temperatures

A critical aspects of this study was to establish the time it would take the smoke coming from the small room—where the fire originated—to heat the padlocks that locked the access door to the main cell, to a temperature that would impede the guards opening them without protective gear.

The heating of a solid object immersed in a hot fluid (smoke in this case) is fundamentally governed by two mechanisms: convective and radiative heat transfer. The former is a result of the temperature difference between fluid and solid, and the corresponding heat flux is expressed as follows,

$$q_c'' = h_c(T_f - T_s), \tag{5}$$

where h_c is the convective heat transfer coefficient, T_f is the fluid temperature, and T_s is the temperature of the solid object. The heat transfer coefficient h_c depends on the geometry and the material of the solid object, and the flow velocity of the hot fluid. Values for h_c can be easily obtained for different shapes, for a given flow field [25]. In the present analysis, the padlocks were assumed to be made of brass and to have a cylindrical shape (with a diameter of 3 cm and a height of 4 cm). The corresponding coefficient was estimated to be 0.51 W/m²·K. This value was compared to the coefficient resulting from a spherical shape, with only negligible differences. It was thus confirmed that a cylindrical shape was an adequate approximation for the purposes of this study.

14

Radiative heat flux is proportional to the difference of the temperatures to the fourth power,

$$q_r'' = \sigma \varepsilon_s (T_f^4 - T_s^4), \tag{6}$$

where σ represents the Stefan-Boltzmann constant ($\sigma = 5.67 \times 10^{-11}$ kW/m^2·K^4), and ε_s is the surface emissivity.

Heat absorbed by the object is transferred into the solid via conduction. Simulating this requires solving a partial differential equation in three dimensions. For thermally thin objects, however, it can be assumed that the body heats up uniformly. Thermally thin objects are defined as objects where the conductive heat transfer into the solid is much faster than the absorbed heat. Whether a body is thermally thin can be verified using Biot's number [25],

$$Bi = \frac{h_c L}{k}, \tag{7}$$

where L is a characteristic length scale (ratio between volume and surface of the cylinder [25]), and k is the thermal conductivity of the material. For bodies with $Bi < 0.1$ it can be assumed that it is thermally thin, and conductive heat transfer into its interior can be neglected. The Biot number for the padlocks was estimated to be around 0.04 (in average), and the heating of the padlocks is thus defined by,

$$\frac{dT_s}{dt} = \frac{A_s}{m_s c} \left(q_c'' + q_r'' \right). \tag{8}$$

Equation (8) is solved for T_s using a finite differences scheme where smoke temperatures and velocities are taken from the CFD smoke movement simulations.

6. Scenario Definition

For the computational domain the entire fourth floor of the prison block was considered, including additionally an empty volume above the block, in order to account for interaction with the environment. Figure 6 shows the computational domain used in the simulations. In order to allow for illustration of interior elements, some external walls were set to "invisible" in the visualisation tool of FDSv5. The bunk beds and sub-divisions made by inmates are also shown

15

(in brown and yellow respectively). Small objects, such as bed frames, are not considered, as they don't have a significant effect on flow simulations.
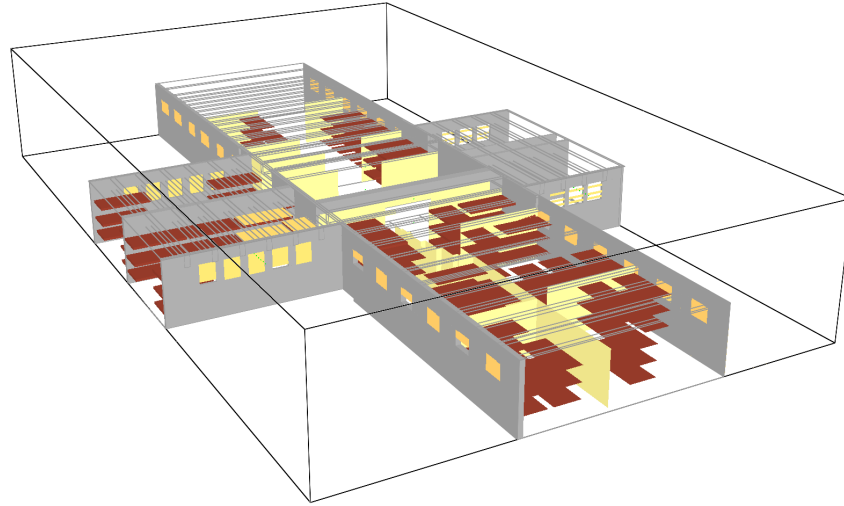

Figure 6: Computational domain.

Given the inherent uncertainties associated with the reconstruction of a catastrophic event, several simulations had to be carried out, taking into account the different possible scenarios. In the following sections an overview of the aspects that define the scenarios is presented.

6.1. Laboratory Tests

In order to obtain a suitable HRR curve as input into the CFD model, laboratory tests were conducted, where the burning behaviour of mattresses identical to the mattresses used in San Miguel prison were analysed.

The HRR of a fire is the result of the combustion of flammable materials that in the growing phases of the fire is intimately linked to the production of fuel. The production rates of fuel are difficult to determine analytically, thus experiments were conducted using oxygen consumption calorimetry. In order to obtain the HRRPUA, small scale experiments were conducted following ASTM-E-1354 [26]. For the estimation of the propagation rate of the spreading front

16

and of the burn out front, large scale experiments were conducted following ASTM-E-1590 [27]. A detailed account of the experiments and the experimental set up can be requested from the authors.

While mattresses will normally be covered by sheets and blankets, due to their small mass, these are very small contributors to the HRR. Thus the HRR was conservatively determined only by the material comprised in the mattress. Sheets and blankets can significantly contribute to the initial spread of the fire, but in absence of reliable information on exactly what amount of combustible material covered the mattress, it was decided to use an uncovered mattress, which represents the scenario with the slowest possible spread rate (and thus the worst case scenario in terms of the analysis being performed). Polyurethane foam can, under certain circumstances, spread a flame much faster than sheets or blankets, but here this is not the case. Typical flame spread velocities for thermally thin materials like sheets or blankets [2] are much greater than those measured for the polyurethane foam mattresses object of this study.

The overall HRR can be divided into two phases; an initial phase, where only the lower mattress burns, and a second phase after the upper mattress is ignited.

The burning area is a function of fundamentally three variables; propagation rate of the spreading front (v_s), propagation rate of the "burn-out" front (v_{BO}), and the "burn-out" time (t_{BO}),

$$
A(t) = \begin{cases}
\dfrac{\pi}{4}(v_s \cdot t)^2 & \text{during phase A} \\[2mm]
\dfrac{\pi}{4}((v_s \cdot t)^2 - (v_{BO} \cdot (t - t_{BO}))^2) & \text{during phase B} \\[2mm]
0.78 v_s \cdot t - \dfrac{\pi}{4}(v_{BO}(t - t_{BO}))^2 & \text{during phase C} \\[2mm]
0.78\,(v_s \cdot t - v_{BO}(t - t_{BO})) & \text{during phase D}
\end{cases}
\tag{9}
$$

The different phases referred to in equation (9) are illustrated in figure 7. The flame spread velocity, the "burn-out" velocity and the "burn-out" time were obtained from large scale experiments (ASTM-E-1590), where samples of the mattresses from the San Miguel prison were burnt. Figure 8 shows photographs
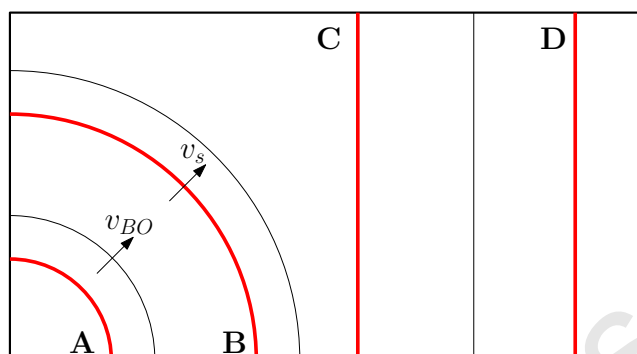
17

Figure 7: Burning phases for lower mattress indicating velocities (v_s and v_{BO}).

taken during the test. The circular shape of the flame front during the initial phase can be clearly appreciated in the image of figure 8(a), while the linear flame front of the later phase is confirmed from the image in figure 8(b). Similar

(a) Flame spread during phase A. (b) Flame spread during phase D.

Figure 8: Steady state flame spread along the sample mattress.

tests were conducted in order to obtain the flame spread velocities of the upper mattress. The parameters resulting from the laboratory experiments are summarised in table 1. Note that the spread rate for the lower mattress was obtained using an isolated mattress, i.e. without re-radiation from items around (especially above the burning region). Since the spread rate increases with increasing external heat flux, the experimentally obtained value is deemed to be lower than the real spread rate. The magnitude of the HRR, calculated using

18

Parameter	Value
HRRPUA	225 kW/m^2
v_s (lower mattresses)	0.001 m/s
v_{BO} (lower mattresses)	0.00013 m/s
v_s (upper mattress)	0.016 m/s
v_{BO} (upper mattress)	0.00045 m/s

Table 1: Summary of parameters obtained for the mattresses tested.

the parameters of table 1 introduced into equations (9) and (2) and considering the sequence of events, is presented in figure 9. The upper mattress is to ignite when the minimum heat flux necessary for ignition is attained. For the tested samples, this heat flux was established as $\dot{q}_{0,ig} = 10 \text{ kW/m}^2$ which was reached when approximately 0.2 m^2 of the lower mattress is burning. If blankets or sheets covering the mattress produce such a burning area during ignition then the first phase, where only one mattress burns, will almost entirely disappear. For the simulations the upper mattress was considered to ignite almost instantly (i.e. starting from phase 2), since the inmates threw an already burning mattress onto the lower level of the bunk bed blocking the access, in order to start the fire in the small room.

The ignition of the first mattress, that is, the process of establishing a stabilised flame big enough to auto-sustain, was carried out by a group of inmates in the main (large) room. Based on this fact and the defenders' objectives of re-creating the events of the fire, once a self-sustained fire was burning, the period of ignition was not considered in the simulations.

6.2. Ventilation conditions

While interviewed inmates stated that windows are generally blocked using cardboard and old mattresses in order to eliminate uncomfortable air currents, it cannot be conclusively affirmed that all windows were blocked at the time of the incident, and that they were kept blocked during the fire (it is reasonable
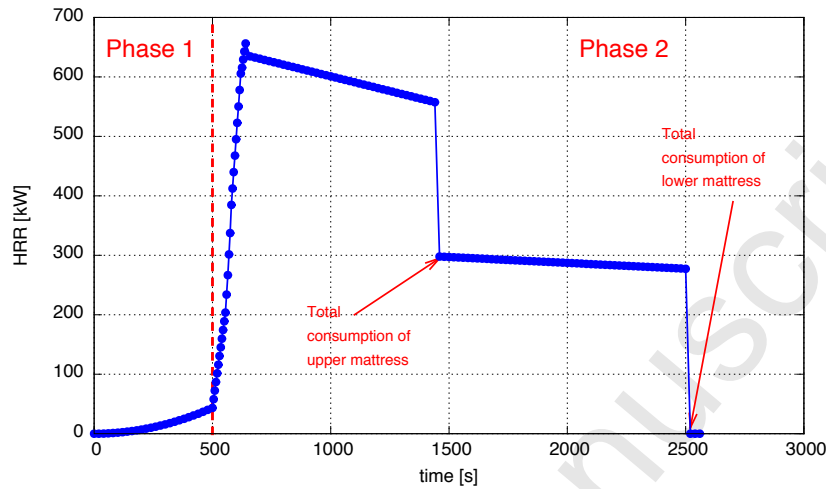
19

Figure 9: Calculated HRR evolution as a function of time for the scenario defined in the experiments.

to believe that inmates would have tried to ventilate the room when it started to fill with smoke). It is, however, clear that the windows of the sanitary room were kept un-blocked at all times (this is common practice among inmates).

As incoming air from the outside could influence the results of the simulations, in one of the simulated scenarios half of the windows of both cells were left un-blocked (windows of the sanitary room were considered un-blocked in all simulations), and the effect was included in the analysis. From meteorological recordings it was established that wind blew westwards with a maximum velocity of 2 m/s, although a scenario without wind was also considered for completeness.

6.3. Simulation time and Fire propagation

The main interest of the present study lied in the early stages of the fire, from ignition up to the time smoke appeared coming out of the sanitary room's windows. There is no doubt that the fire, which originated in the small adjacent cell, eventually spread to the main cell resulting in a maximum HRR much higher than the HRR presented in figure 9 (which only considered the mattresses

20

of one bunk bed without cover), or indeed the 2.4 MW estimated from equation (3). However, it was deemed that the initial fire alone would produce enough smoke in short enough time, so that for the purpose of this analysis the main cell could be considered inert. As an additional conjecture it was considered that 600 seconds would be enough to replicate smoke coming out of the sanitary room windows across the large room. The simulations confirmed both conjectures, so that no additional simulation time had to be added.

6.4. Flashover

As indicated in section 4, a post-flashover fire is controlled by the ventilation conditions of the compartment. Thus, the curve of fire size (figure 9) was only used before the small room attained flashover conditions. After flashover, the maximum HRR of 2.4 MW was estimated using equation (3), where the vents considered were the windows of the small room, and the opening towards the main cell.

The inherent difficulty of simulating fire spread and the resulting growth rate of the fire using a CFD based fire model such as FDSv5 with a relatively coarse grid, also limits its capability of predicting the transition from a pre-flashover to a post-flashover fire [22]. However, the model can give indications as to the time when flashover will occur. A possible criterion for the occurrence of flashover is that the oxygen concentration at the height of the initially burning object descends significantly (from an average of 13.5% in the pre-flashover stage to about 8.5% during post-flashover [8, 9]). The average of both numbers, 11%, was used to determine the onset of flashover. This value can be obtained as an output from FDSv5. Thus a first set of simulations was run up to the moment defined by this criterion, and the elapsed time was noted. A sensitivity analysis around this time was conducted varying the oxygen concentration within the range indicated above and also using other flashover criteria [2]. The rate of change is so fast at this stage of the fire that the time difference can be considered negligible compared to other variables of the problem. The simulations were then restarted using the maximum HRR defined in the previous

21

paragraph. Flashover times for the scenarios considered in this study ranged between 190 seconds and 320 seconds, depending on ventilation conditions and openings. These times compared well to the time estimated from simple two-zone calculations, where the time to flashover was defined as the time it took the smoke layer to descend to 0.5 m (the height of the burning mattress), which happened after about 170 s. Note that the longer pre-flashover period obtained from CFD calculations resulted in a more conservative overall estimate.

7. Simulation Results

In all simulated scenarios (blocked and un-blocked windows, wind and no wind) the flashover criterion was reached between 230 and 290 seconds after ignition using the HRR from figure 9 as input. Although there is no evidence from the fire incident to validate these numbers, fires of similar characteristics in similar compartments have shown to transition to flashover in comparable times. Abecassis-Empis *et al.* report secondary ignition 275 second into the fire at the Dalmarnock Fire Tests, and flames projecting into corridor 30 seconds later ([28]). The fresh air supply in the small room produced a fire of about 2.4 MW after flashover, according to equation (3).

7.1. Smoke movement and temperature distributions

Figure 10 shows the distribution of smoke across the floor in a simulation of the scenario with blocked windows. The smoke is coming from the small room where the fire initiated, and it can be seen that 90 seconds after ignition most of the smoke is still contained in this compartment (figure 10(a)). Four minutes later (i.e. 330 seconds after ignition) smoke has spread to the entire cell, and is filling the adjacent cell as well.

Figure 11 shows an external view of the simulated prison, where the roof of the main room can be seen to the left of the sanitary room. This view is approximately the same as the view from the CCTV cameras that recorded the first smoke appearance. At 90 seconds into the simulated fire, there is no

22
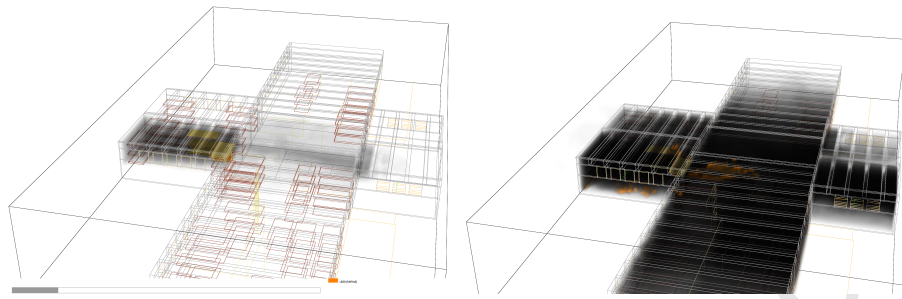
(a) Simulated smoke distribution 90 seconds after ignition.

(b) Simulated smoke distribution 330 seconds after ignition.

Figure 10: Simulated smoke distribution across the compartment.

smoke visible at the sanitary room windows (figure 11(a)), which is consistent with the smoke distribution shown in figure 10(a). Less than four minutes later (310 seconds into the simulated fire) thick smoke can be seen coming out of the windows (11(b)). Although it is somewhat complicated to quantitatively assess a visual criterion ("first smoke seen in CCTV recordings"), thick smoke as seen in figure 11(b) can clearly be regarded as visible, thus it can be concluded that simulated smoke presence after 310 seconds would be at least as intense as recorded by CCTV. In the simulations, the percentage of obscuration through the smoke outside the sanitary room windows was recorded as a proxy for smoke visibility, and in all simulated scenarios the obscuration exceeded 90% shortly after 300 s.

The ceiling slab is supported by parallel beams that cross the main cell with a distance of approximately 0.5 m between them. The beams are 0.5 m high, thus forming channels for the smoke to flow across the room, from the small room to the sanitary room. This partially explains the rapid appearance of smoke in the sanitary room. The temperature distribution and flow pattern along the channel formed by the beams is illustrated in figure 12, approximately 240 s into the fire. Figure 12(a) shows a longitudinal temperature distribution along the centre-line of the main room. The high temperatures in the beam-channel that connects the small room with the sanitary room can be seen. The

23

(a) View of the sanitary room windows, 90 seconds into the simulation.

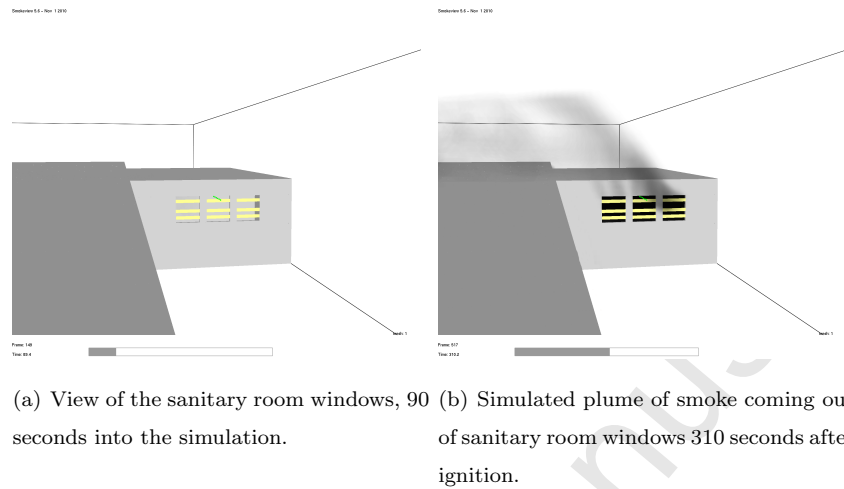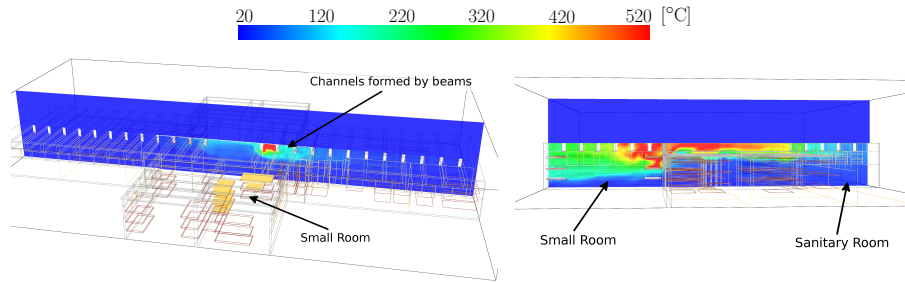(b) Simulated plume of smoke coming out of sanitary room windows 310 seconds after ignition.

Figure 11: External view of the simulated smoke appearance at the sanitary room window. The thin lines indicate the limits of the computational domain.

temperatures towards the rear of the main room remain largely unaffected. Figure 12(b) shows the temperature distribution on a plane cutting through the beam-channel, with the small room to the left (where the fire initiates), and the sanitary room to the right. The high temperatures in the small room (over 300°C), and the unobstructed flow of hot gases (smoke) going from the small room to the sanitary room can be appreciated. It should also be noted that the simulated temperatures (with a maximum of about 520°C) are lower than the maximum temperature obtained from the simple heat balance of section 4.1 (750°C). This can be attributed to external flaming, which is not considered in equation (4).

7.2. Padlock temperatures

Figure 13 shows the smoke temperature and the temperature evolution of the padlocks that locked the main cell door, according to equation (8). The maximum smoke temperature, reached after flashover, was of about 500°C, which is considerably lower than the temperature estimated from the energy balance described in equation (4) (750°C).

24

20   120   220   320   420   520 [°C]

Channels formed by beams

Small Room

Small Room   Sanitary Room

(a) Temperature distribution across the middle of the prison block.

(b) Temperature distribution across the small room, the main cell and the sanitary room..

Figure 12: Temperature distribution across the computationl domain.

The upper padlock, at 2.5 m above the floor, was immersed in the hot gases flowing from the fire compartment to the sanitary room, and thus its temperature started rising soon after ignition of the fire. Only 100 seconds after the fire started, the temperature already was above 100°C. By the time the fire was noted by the guards (according to previous paragraphs around five minutes after it started) the temperature of the upper padlock exceeded 400°C. The lower padlock, at 0.5 m above the floor, received lesser heat flux, and its
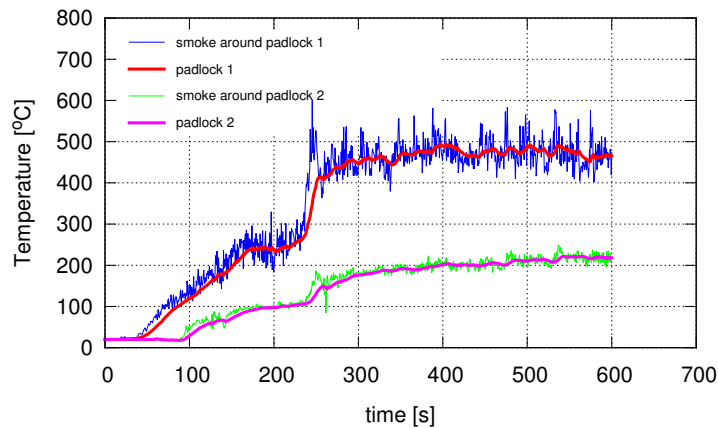

Figure 13: Padlock temperatures.

temperature rose less quickly, remaining below 200°C until the time the fire was

25

noted.

In all cases it is clear that the temperature of the padlock rose to values that will make the padlock impossible to handle by hand. There is no reliable data available on the operability of padlocks at high temperature or on thresholds that enable people to handle objects at high temperature, therefore it is best not to provide a prediction of the time where it became impossible to handle the padlock and only accept that this threshold would have been attained before the fire was detected.

8. Discussion and Conclusions

The simulations were set up in a manner such that the results would be conservative (i.e. they would yield the longest reasonable time between sustained ignition, and smoke appearing at the windows of the sanitary room, under any rational assumptions that fit the evidence), in order to account for all uncertainties associated with modelling a physical phenomenon. It is beyond doubt that a fire, once established on the mattress, would burn considerably faster than the results obtained from the laboratory experiments (since the mattresses were considered to be uncovered, with no additional fuel). But even so the simulations showed that smoke from the fire would have exited the windows of the sanitary room little over five minutes after ignition. Thus, when the first smoke appeared in the CCTV recordings of the camera outside the sanitary room windows, the fire could not have been burning for longer than the five minutes obtained from the simulations. This confirms that the guards did not knowingly ignore the fire for a considerable amount of time.

The simulations also showed that the temperature of the padlocks were much higher than what could be handled without protective gear by the time the guards arrived at the cell door.

26

References

[1] J. Moncada, Lessons of Comayagua, NFPA Journal, September/October (2012).

[2] D. Drysdale, An Introduction to Fire Dynamics, 3rd Edition, ISBN 0-470-31903-8, Wiley & Sons, New York, 2011.

[3] V. Babrauskas, R. Peacock, Heat Release Rate: The Single Most Important Variable in Fire Hazard, Fire Safety Journal 18 (3) (1992) 255–272. `doi:10.1016/0379-7112(92)90019-9`.

[4] V. Babrauskas, Heat Release Rates, in: P. DiNenno (Ed.), SFPE Handbook of Fire Protection Engineering, 3rd Edition, National Fire Protection Association, Quincy, MA 02269, 2002, Ch. 3-1, pp. 3–1–3–37.

[5] A. Heselden, P. Thomas, M. Law, Burning rate of ventilation controlled fires in compartments, Fire Technology 6 (2). `doi:10.1007/BF02588898`.

[6] E. Zukoski, Development of a Stratified Ceiling Layer in the Early Stages of a Closed–room Fire, Fire and Materials 2 (2). `doi:10.1002/fam.810020203`.

[7] W. Walton, Zone Computer Fire Models for Enclosures, in: P. DiNenno (Ed.), SFPE Handbook of Fire Protection Engineering, 3rd Edition, National Fire Protection Association, Quincy, MA 02269, 2002, Ch. 3–7, pp. 3–189–3–193.

[8] C. L. Beyler, Ignition and Burning of a Layer of Incomplete Combustion Products, Combustion Science and Technology 39 (1-6) (2007) 287–303. `doi:10.1080/00102208408923793`.

[9] C. L. Beyler, Major species production by diffusion flames in a two-layer compartment fire environment, Fire Safety Journal 10 (1) (1986) 47–56. `doi:10.1016/0379-7112(86)90031-7`.

27

[10] Novozhilov, Computational fluid dynamics modeling of compartment fires, Progress in Energy and Combustion Science 27 (6) (2001) 611–666. `doi:` `10.1016/S0360-1285(01)00005-3`.

[11] J. Ferziger, M. Perić, Computational Methods for Fluid Dynamics, Springer, 1996.

[12] T.-S. Shen, Y.-H. Huang, S.-W. Chien, Using fire dynamic simulation (FDS) to reconstruct an arson fire scene, Building and Environment 43 (6) (2008) 1036–1045. `doi:10.1016/j.buildenv.2006.11.001`.

[13] O. Delémont, J.-C. Martin, Application of computational fluid dynamics modelling in the process of forensic fire investigation: problems and solutions., Forensic science international 167 (2-3) (2007) 127–135. `doi:` `10.1016/j.forsciint.2006.06.053`.

[14] K. McGrattan, B. Klein, S. Hostikka, J. Floyd, Fire Dynamics Simulator (Version 5) – User's Guide, NIST Special Publication 1019–5 (2008).

[15] K. McGrattan, S. Hostikka, J. Floyd, H. Baum, R. Rehm, Fire Dynamics Simulator (Version 5) – Technical Reference Guide, NIST Special Publication 1018–5 (2010).

[16] J. Smagorinsky, General Circulation Experiments with the Primitive Equations, Monthly Weather Review 91 (3) (1963) 99–164. `doi:10.1175/` `1520-0493(1963)091<0099:GCEWTP>2.3.CO;2`.

[17] Verification and Validation of Selected Fire Models for Nuclear Power Plant Applications, Volume 7: FDS, U.S. Nuclear Regulatory Commission, Office of Nuclear Regulatory Research (RES), Rockville, MD, and Electric Power Research Insititute (EPRI), Palo Alto, CA, NUREG–1824 and EPRI 1011999 (2007).

[18] J. G. Nielsen, Validation Study of Fire Dynamics Simulator, Master's thesis, Aalborg University, Denmark (2013).

28

[19] J. Kwon, N. Dembsey, C. Lautenberger, Evaluation of FDS v.4: Upward Flame Spread, Fire Technology 43 (4) (2007) 255–284. `doi:10.1007/s10694-007-0020-x`.

[20] G. Rein, J. Torero, W. Jahn, J. Stern-Gottfried, N. Ryder, S. Desanghere, M. Lazaro, F. Mowrer, A. Coles, D. Joyeux, A. D., J. Capote, A. Jowsey, C. Abecassis-Empis, P. Reszka, Round–Robin Study of *a priori* Modelling Predictions of the Dalmarnock Fire Test One, Fire Safety Journal 44 (4) (2009) 590–602. `doi:10.1016/j.firesaf.2008.12.008`.

[21] B. Karlsson, J. Quintiere, Enclosure Fire Dynamics, 1st Edition, ISBN 0-8493-1300-7, CRC Press, London, New York, 2000.

[22] W. Jahn, G. Rein, J. Torero, The effect of model parameters on the simulation of fire dynamics, Fire Safety Science 9 (2008) 1341–1352. `doi:10.3801/IAFSS.FSS.9-1341`.

[23] W. Jahn, G. Rein, J. Torero, A posteriori modelling of the growth phase of Dalmarnock Fire Test One, Building and Environment 46 (5) (2011) 1065–1073. `doi:10.1016/j.buildenv.2010.11.001`.

[24] L. H. Hu, N. K. Fong, L. Z. Yang, W. K. Chow, Y. Z. Li, R. Huo, Modeling fire-induced smoke spread and carbon monoxide transportation in a long channel: Fire Dynamics Simulator comparisons with measured data., Journal of hazardous materials 140 (1-2) (2007) 293–8. `doi:10.1016/j.jhazmat.2006.08.075`.

[25] F. Incropera, D. DeWitt, Fundamentals of Heat and Mass Transfer, 4th Edition, Wiley & Sons, New York, 1996.

[26] ASTM Standards, ASTM E1354 – Standard Test Method for Heat and Visible Smoke Release Rates for Materials and Products Using an Oxygen Consumption Calorimeter (2010).

[27] ASTM Standards, ASTM E1590 - Standard Test Method for Fire Testing of Mattresses (2007).

29

[28] C. Abecassis-Empis, P. Reszka, T. Steinhaus, A. Cowlard, H. Biteau, S. Welch, G. Rein, J. L. Torero, Characterisation of Dalmarnock fire Test One, Experimental Thermal and Fluid Science 32 (2008) 1334–1343. doi:10.1016/j.expthermflusci.2007.11.006.

30